Self-Propelled Jumping Upon Coalescence on Leidenfrost Surfaces

by

Fangjie Liu

Department of Mechanical Engineering and Materials Science
Duke University

Date: _____

Approved:

_____
Chuan-Hua Chen, Supervisor

_____
Thomas P. Witelski

_____
Pei Zhong

Thesis submitted in partial fulfillment of the requirements for the degree of Master of Science in the Department of Mechanical Engineering and Materials Science
in the Graduate School of Duke University
2013

Abstract

Self-Propelled Jumping Upon Coalescence on Leidenfrost Surfaces

by

Fangjie Liu

Department of Mechanical Engineering and Materials Science
Duke University

Date: _____

Approved:

_____
Chuan-Hua Chen, Supervisor

_____
Thomas P. Witelski

_____
Pei Zhong

An abstract of a thesis submitted in partial fulfillment of the requirements for the degree of Master of Science in the Department of Mechanical Engineering and Materials Science
in the Graduate School of Duke University
2013

Abstract

When two drops coalesce on a superhydrophobic surface, the merged drop spontaneously jumps out of plane. This self-propelled jumping has been observed on many biological and synthetic superhydrophobic surfaces, with potential applications in self-cleaning materials and self-sustained condensers. The jumping is powered by surface energy released upon coalescence and the velocity follows a capillary-inertial scaling. However, two puzzles remain to be solved: (i) The jumping velocity is significantly smaller than the capillary-inertial velocity, which corresponds to a very low conversion efficiency from surface to kinetic energy; (ii) The capillary-inertial scaling is no longer valid below a critical radius, and jumping is no longer observed upon coalescence of drops well below the cut-off radius.

To investigate these puzzles, a Leidenfrost collider was constructed on which drops floating on a vapor layer were guided to merge and subsequently jump on a heated substrate. The jumping velocity upon symmetric coalescence of equally-sized drops was observed to follow the capillary-inertial scaling, and the non-dimensional jumping velocity of approximately 0.2 on Leidenfrost surfaces was consistent with that on superhydrophobic surfaces. Asymmetric coalescence on Leidenfrost surfaces led to a smaller non-dimensional jumping velocity, but the overall trend was still consistent with the capillary-inertial scaling. Unlike superhydrophobic surfaces, we did not observe an obvious cut-off for coalescing drops with a radius down to 20 μm, the lowest accessible to the Leidenfrost collider. When compared with a phase-field

numerical simulation, the Leidenfrost experiments confirmed the capillary-inertial mechanism leading to the self-propelled jumping.

Contents

List of Figures

Acknowledgements

First, I would like to thank my advisor, Professor Chuan-Hua Chen for his guidance and insights and for always being there when I was stuck. In addition, I thank Professor Pei Zhong and Professor Thomas Witelski for serving on my committee. I would also like to thank our collaborators, Professor James Feng and Giovanni Ghigliotti for all the discussions and help on the simulation work. Furthermore I would like to thank Jonathan Boreyko for his work at the initial phase of the project as well as his encouragement. I also thank my colleagues who are always very considerate and bear with the noise during the experiment, especially Xiaopeng Qu who always offers to help move the instruments. I am very grateful to Bernie Jelinek in the Physics machine shop and John Goodfellow in the MEMS machine shop for help with the machining of the device.

I would also like to express my thanks to the following funding agencies for their support: the National Science Foundation (CBET-08-46705 and CBET-12-36373) and the Defense Advanced Research Projects Agency (N66001-10-1-4048).

My sincere thanks also goes to my roommate and friend, Lei Tang, for her continuous emotional support in both my work and life. Last, but not least, I would like to thank my boyfriend and my family for their understanding and support as always.

1

Introduction

When two drops coalesce on a superhydrophobic surface, the merged drop self-propels itself to jump perpendicular to the surface (Boreyko and Chen, 2009). The jumping motion is powered by the surface energy released upon drop coalescence, and the out-of-plane direction results from the counter action of the superhydrophobic substrate to the impingement of the liquid bridge connecting the coalescing drops (Boreyko and Chen, 2009, 2010). The self-propelled jumping has been reported on a variety of natural water-repellant surfaces, including those on spring tails, lacewings, and cicadas (Helbig et al., 2011; Watson et al., 2011; Wisdom et al., 2013). For engineering applications, the jumping motion has been applied to develop superhydrophobic surfaces that are anti-dew (Boreyko and Chen, 2009; Enright et al., 2012; Feng et al., 2012; Rykaczewski et al., 2012), anti-icing (Boreyko and Collier, 2013; Zhang et al., 2013) or self-cleaning (Wisdom et al., 2013), as well as heat transfer systems that enhance dropwise condensation (Chen et al., 2007; Dietz et al., 2010; Cheng et al., 2012; He et al., 2012; Miljkovic et al., 2013) and promote thermal rectification (Boreyko et al., 2011; Boreyko and Chen, 2013).

Despite many applications of the jumping phenomena, the understanding is more

or less limited to a primitive capillary-inertial scaling law based on an energetic argument (Boreyko and Chen, 2009). When two equally sized drops of radius r_0 coalesce into a larger one (figure 1.1), the equilibrium radius is $r = 2^{\frac{1}{3}} r_0$ by mass conservation. The released surface energy is proportional to the reduced surface area, $\Delta E_s = 4\sigma\pi r_0^2(2 - 2^{\frac{2}{3}})$, where σ is surface tension of the air-liquid interface. The joint drop has a mass of $m = \frac{8}{3}\rho_L \pi r_0^3$ where ρ_L is the density of the liquid. The presence of the substrate breaks the symmetry of energy release (figure 1.1) and the joint drop eventually jumps up with an average velocity $\bar{v}_j = \bar{v}_{j,z}$, where the velocity only has vertical z-component for symmetric coalescence. If all the released surface energy were converted to kinetic energy, the merged drop might achieve a maximum possible jumping velocity, $\bar{v}_s = \sqrt{2\Delta E_s/m} = 1.11 u_{ci}$, where u_{ci} is the capillary-inertial velocity,

$$u_{ci} = \sqrt{\frac{\sigma}{\rho_L r_0}}. \tag{1.1}$$

Note that the maximum jumping velocity assuming perfect energy conversion efficiency is very close to the capillary-inertial velocity scale, $\bar{v}_s \approx u_{ci}$. The capillary-inertial scaling trend in equation (1.1) was indeed confirmed by measurements of coalescing condensate drops of different radii on superhydrophobic surfaces in figure 1.2 (Boreyko and Chen, 2009), however, two puzzles remain to be solved: (i) The jumping velocity of the merged drop $\bar{v}_j$ is significantly smaller than the capillary-inertial scale, $\bar{v}_j \approx 0.2 u_{ci}$; In terms of the energy conversion efficiency, the kinetic energy associated with the jumping motion was less than 4% of the total released surface energy, $\frac{1}{2} m \bar{v}_j^2 \lesssim 4\% \Delta E_s$. (ii) On superhydrophobic surfaces, the capillary-inertial scaling was no longer observed when the drop radius was below a threshold of around 30 μm; This threshold is well above the 10 nm length scale based on $Oh \sim 1$, where the Ohnesorge number Oh denotes the relative importance of viscous effects against the

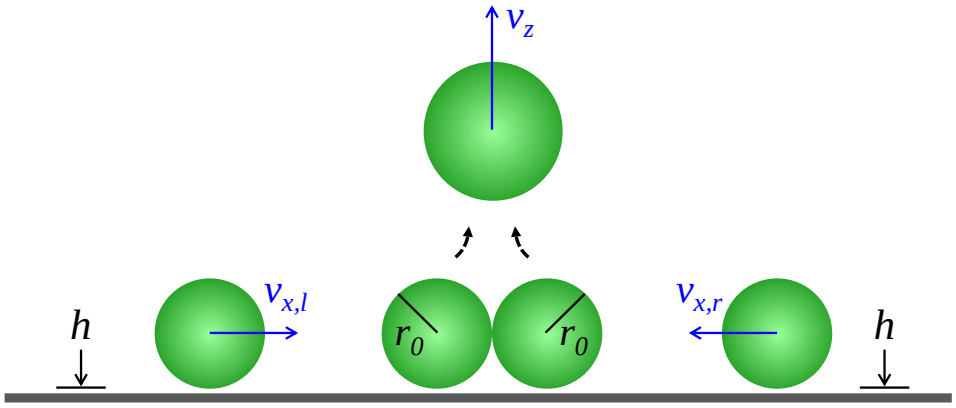

FIGURE 1.1: Schematic of the drop coalescence process: on a Leidenfrost surface, two drops approach each other at velocities of $v_{x,l}$ and $v_{x,r}$ with an initial radius r_0 and then coalesce into a larger spherical drop with an equilibrium radius of $r = 2^{\frac{1}{3}} r_0$. The reduction in surface area releases excess surface energy, powering the merged drop to jump away from the substrate. The vapor layer thickness is h and the jumping velocity is v_z , which is perpendicular to the substrate.

capillary-inertial effects,

$$Oh = \frac{\mu_L}{\sqrt{\rho_L \sigma r_0}}, \tag{1.2}$$

where μ_L is the liquid viscosity.

These remaining puzzles on the jumping velocity and cutoff radius are of practical interest. For example, in designing vapor chambers using the jumping drops for liquid return, the jumping velocity is critical for evaluating the distance the self-propelled drops can travel against gravity to ensure orientation independence (Boreyko and Chen, 2013); in designing superhydrophobic condensers using the jumping drops for condensate removal, the cutoff radius is crucial for determining the average size of the condensate drops before they are removed by jumping (Miljkovic and Wang, 2013).

To address these remaining puzzles, we studied the self-propelled jumping on Leidenfrost surfaces (figure 1.1), which approximate the superhydrophobic surfaces but offer a few distinct advantages. A Leidenfrost surface is a surface heated to a

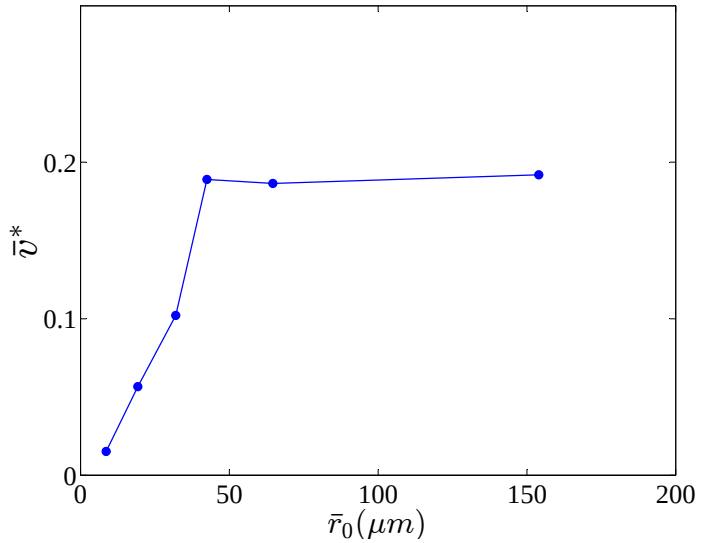

FIGURE 1.2: Non-dimensional velocity vs radius of jumping condensate drops. $\bar{v}^*$ is non-dimensionalized by u_{ci}. Data taken from Boreyko and Chen (2009) where only data with drop radii disparity within 33% were used. (i) The jumping velocity of the merged drop $\bar{v}^* \approx 0.2$; In terms of the energy conversion efficiency, the kinetic energy associated with the jumping motion was less than 4% of the total released surface energy. (ii) The capillary-inertial scaling was no longer observed when the drop radius was below a threshold of around 30 μm.

temperature (Leidenfrost Point) significantly above a liquid's boiling point. Once a drop is in contact with the surface, an insulating vapor layer is immediately formed between the drop and the surface (Biance et al., 2003). The drop sits on the vapor layer resembling perfect superhydrophobicity with a contact angle of 180°. The advantages of Leidenfrost surfaces include: (i) the drop size and coalescence process are easier to control through variations in drop generation methods; (ii) the vapor layer simplifies the model by eliminating drop-surface interaction and moving contact lines.

There are two caveats associated with the Leidenfrost setup: the approaching velocity of the two drops ($v_{x,l}, v_{x,r}$ prior to coalescence in figure 1.1) and the effects of vapor layer. These effects can be assessed by the Weber number, We, which

denotes the relative importance of inertia versus capillarity,

$$We = \frac{\rho v^2 r_0}{\sigma}, \tag{1.3}$$

where v is the characteristic velocity of the moving drop. In our experiment, care was taken to ensure that the jumping velocity after the coalescence was not significantly affected by approaching velocities. We ensured that in our experiment the Weber number was consistently below unity based on the relative approaching velocity ($v_{x,a}$) which is a sum of the horizontal velocities of the two drops approaching from the left and right, $v_{x,a} = v_{x,l} - v_{x,r}$ (figure 1.1). This low Weber number regime resembles "regime I" in Qian and Law (1997); Tang et al. (2012) where two drops always coalesce. As far as the self-propelled jumping motion is concerned, we are by default in the low-Weber number regime ($We \lesssim 1$) with $v \lesssim u_{ci}$. The vapor layer can be approximated as a passive medium simply imposing a non-wetting boundary condition, i.e. an idealized solid surface with which a liquid drop is touching at a contact angle of 180° (Biance et al., 2006).

In this paper, we will first present our experimental methods to generate self-propelled jumping upon coalescence on Leidenfrost surface. We then analyze the jumping process and extract the jumping velocity upon drop coalescence. Finally, we will discuss the non-dimensional velocity and cut-off radius, and compare the experimental results with a numerical model.

2

Methods

On Leidenfrost surfaces, the out-of-plane jumping velocity was measured for drop radii varying more than one order of magnitude. To obtain such a large range, we employed a few variations to our experimental setup depending on the desired drop radius. Note that two drops approaching on the Leidenfrost collider do not necessarily coalesce (Neitzel and Dell'Aversana, 2002), an example being non-coalescing water and ethanol drops upon collision (Boreyko, 2012). However, when the two drops are made of water and the approaching velocity is small ($We \lesssim 1$), coalescence was always observed. Other working fluids are also possible to obtain coalescence induced jumping on a Leidenfrost surface(Boreyko, 2012), but more difficult than water. Therefore, we only use water in our experiments.

To obtain coalescence of relatively large drops, deionized water droplets were released from opposite sides of an aluminum surface heated above the Leidenfrost point at which drops float on a vapor layer (figure 2.1 and 2.2). Two grooved tracks, each with a width of 2 mm and a slanting angle of 5°, were used to guide the motion of the floating drops. A cartridge heater was inserted beneath the Leidenfrost surface and powered through a temperature controller (Omega CNi3243). The temperature

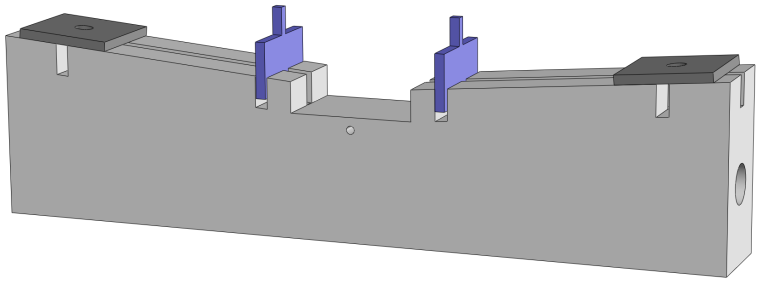

FIGURE 2.1: Schematic of the Leidenfrost surface for drop coalescence on a heated aluminum stage, the flat region in the center extended to a slanted ramp on each side.The ramps were grooved into the aluminum stage, each with a length of 15 mm, a width of 2 mm, and a height of 5 mm. The entire stage was heated by two cartridge heaters inserted beneath each ramp, and the temperature of the flat center surface was monitored by a thermocouple inserted 2 mm underneath. The flat center region had a length of 20 mm and a width of 15 mm.

of the Leidenfrost surface was measured by a K-type thermocouple inserted 2 mm beneath the surface where coalescence occurred. The Leidenfrost surface was heated to be 250 $\pm 1^{\circ}$C, significantly higher than the measured Leidenfrost point of 195 $^{\circ}$C for deionized water drops. Note that both temperatures were measured by the inserted thermocouple, so the temperatures of actual surface should be somewhat lower. The coalescence process was recorded by a high-speed camera (Phantom V7.1 or V710) attached to a long-distance microscope (Infinity K2). Typical frame rate are 800 fps or 1000 fps but at times higher frame rate such as 6000 fps were also used to capture much detailed process. The exposure time was kept below 10% of the frame interval.

The Leidenfrost surface for drop coalescence was a heated aluminum stage, with the flat region in the center extended to a slanted ramp on each side (figure 2.1). The ramps were grooved into the aluminum stage, each with a length of 15 mm, a width of 2 mm, and a height of 5 mm. The entire stage was heated by two cartridge heaters inserted beneath each ramp, and the temperature of the flat center surface was monitored by a thermocouple inserted 2 mm underneath. The flat center region had a length of 20 mm and a width of 15 mm. In the "colliding" mode, drops were

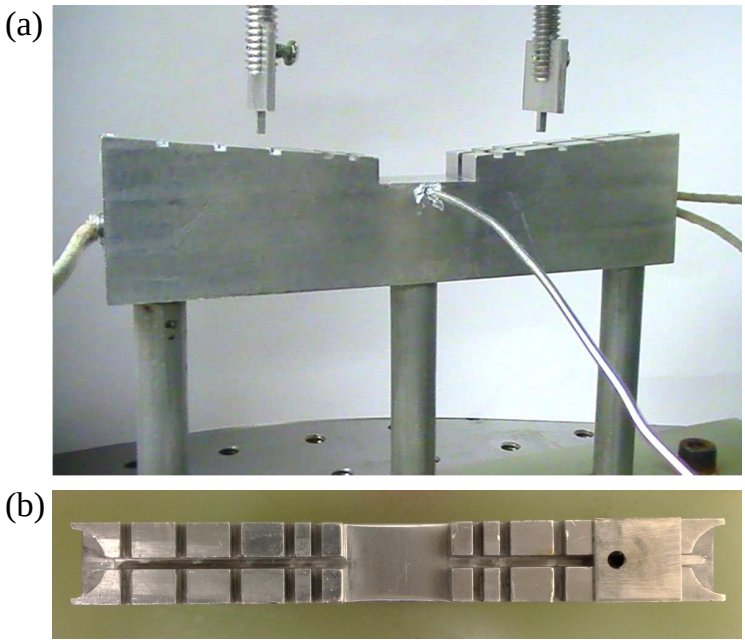

FIGURE 2.2: The aluminum stage was fixed to the optical table with an insulating plastic inbetween. The entire stage was heated by two cartridge heaters inserted beneath each ramp, and the temperature of the flat center surface was monitored by a thermocouple inserted 2 mm underneath. Thermal grease was applied in the hole. In the "colliding" mode, the two gates were lowered down into corresponding slots and drops were released from behind the gates. In the "exploding" mode, the gates were lifted away from the collider and a large drop was deposited on a holed plate placed above the grooved track shown on the right, and the drop exploded into small droplets upon boiling. In the "gating" mode, the gates were lowered with a fixed gap between the bottom of the gates and the bottom of the groove. A large drop was placed behind one of the gates. Two gate positions were used to obtain different approaching velocity in the "colliding" mode.

released from behind two electronically controlled gates. In the "exploding" mode, a large drop was deposited on a holed plate placed above the grooved track, and the drop exploded into small droplets upon boiling. In the "gating" mode, a large drop was placed behind one of the gates, with a fixed gap of between the bottom of the gate and the bottom of the groove. Depending on the desired diameter of drop, the gap dimension was varied from 20 to 200μm. Two positions were used for the gates, 0.5 cm and 4 cm from the center to edge.

Three variations of the setup were used depending on the desired range of drop

radii. (i) For $r_0 \gtrsim 300$ μm, a Leidenfrost drop "collider" was used (figure 2.2). Water drops of a desired volume were pipetted behind two initially closed gates, which were lifted up by solenoid actuators (Pontiac Coil L-04PL012D-C) to simultaneously release the drops. (ii) For 100 μm $\lesssim r_0 \lesssim$ 300 μm, a drop "exploder" was used. An aluminum plate with a 3 mm-radius hole was placed on top of the grooved track. Since the plate was far away from the heated surface, its temperature was below the Leidenfrost point but above the boiling point of water. A drop with a diameter larger than the hole was deposited onto the hole. Because of boiling, the large drop exploded into smaller droplets, which in turn passed through the hole and slid down the tracks to the horizontal Leidenfrost surface in the middle. Since many tiny droplets were produced, particularly if a syringe was used to supply a stream of large drops, only one track was needed for drop coalescence to be captured. (iii) For $r_0 \lesssim 100$ μm, a drop "gate" was used. A small gap was maintained between the aluminum gate and the bottom surface of the grooved track. Depending on the desired diameter of drop, the gap dimension was varied from 20 to 200μm. Since the gap inhibited the heating of the gate, the gate was below the Leidenfrost point, and a drop deposited behind the gate again experienced explosion because of boiling. Among the droplets generated, only those with diameters smaller than the gap height could pass through to reach the Leidenfrost surface of interest. For the gating method, measurements were excluded when intermittently strong vapor flow associated with the explosion was detected. To avoid interference of the vapor flow, droplets were generated from only one gate.

3

Results

We obtained coalescence on Leidenfrost surfaces for drop radii varying more than one order of magnitude. In this chapter, we will analyze the jumping process and extract jumping velocity of Leidenfrost drops upon coalescence, and then discuss the limit of accessible drop radii in our experiment.

3.1 Jumping velocity

A representative jumping process obtained by the "colliding" mode is shown in figure 3.1. In this particular video, the second drop on the right coalesce from behind with an angle of approximately 45°(the approaching velocity 0.09m/s). The most important feature is the rapidly expanding liquid bridge connecting the two drops, as the impingement of the liquid bridge against the substrate and the associated counter force leads to the eventual out-of-plane jumping.

A representative jumping process obtained by the "gating" mode is shown in figure 3.2, which overlays the time-lapsed images of the jumping event. The small droplets decelerate in air as a consequence of air friction in addition to gravity.

The out-of-plane jumping velocity for both large and small drops can be fitted

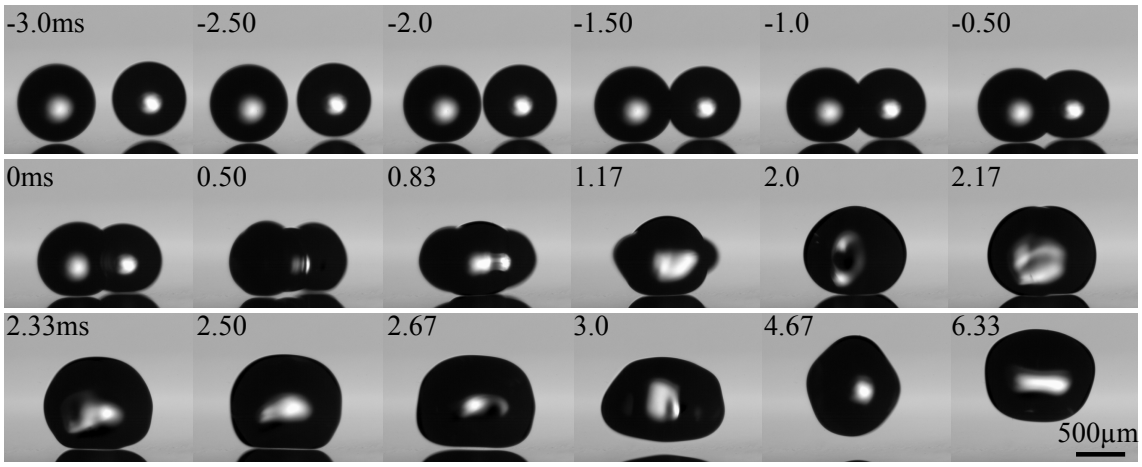

FIGURE 3.1: Jumping process on a Leidenfrost surface upon coalescence of drops with an average radius of 380 μm. Left drop (390μm) is moving at 0.065 m/s and right drop(370μm) at 0.09 m/s. They approach each other at an angle of approximately 45° from the optical axis. At 0 ms, a liquid bridge is formed between the drops which eventually impinges the bottom substrate. The interaction between the merged drop and the substrate eventually lead to the upward jumping motion, with the merged drop departing the surface around 2.67 ms , at an average velocity of 0.076 m/s.

to a second order polynomial. In figure 3.3, the measured velocity is plotted as a function of the initial average radius ($\bar{r}_0$) of the coalescing drops. For nearly symmetric coalescence, the jumping velocity was dominated by the z-component, $\bar{v} \approx \bar{v}_z$. To accurately extract the initial departure velocity from the trajectory of the merged drop, this deceleration must be taken into account for both larger drops as in figure 3.1 and smaller drops as in figure 3.2. In the case of very large drop radii($r \geqslant 141\mu m$, $\frac{v_0/\tau_v}{g} \leqslant 1$), the deceleration is dominated by gravity,

$$z = v_0 t - \frac{1}{2} g t^2, \tag{3.1}$$

where g is the gravitational constant. In the case of very small drop radii($r \leqslant 141\mu m$,$\frac{v_0/\tau_v}{g} \geqslant 1$), the decelerating trajectory is dominated by the viscous drag in the air. The Reynolds number($Re = \rho_G v \bar{r}_0/\mu_G$) is always less than unity when

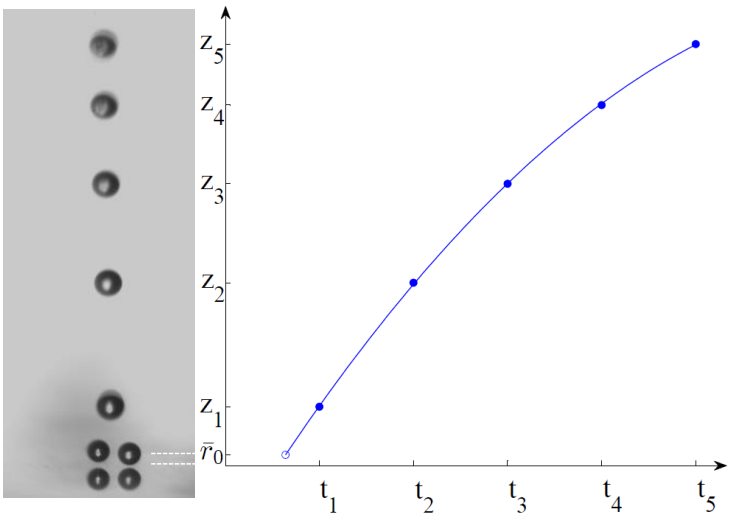

FIGURE 3.2: Trajectory of the self-propelled jumping upon coalescence of drops with an average initial radius of 22 μm. (a) The jumping process illustrated by overlaid images taken at a time interval (δt) of 1250 μs. Note that the drop on the left is slightly out of focus, approaching the other drop from behind. (b) The jumping velocity is extracted based on the first three recorded locations of the merged drop immediately after the launching, z_1, z_2 and z_3 taken at a time interval δt. The location of the Leidenfrost surface is fixed by the mirror image of the drop(s) in focus, and the subsequent locations are measured with respect to the Leidenfrost surface. A parabolic fitting to the first three data points are used to extract the jumping velocity at z_1, which is lower bounded by the average velocity between z_1 and z_2, and upper bounded by the velocity extrapolated to a vertical location corresponding to the center of mass of the initial drops.

$r \leqslant 141\mu m$, thus we have

$$z = v_0\tau_v\left(1 - e^{-\frac{t}{\tau_v}}\right) = v_0\tau_v\left(\frac{t}{\tau_v} - \frac{1}{2}\frac{t^2}{\tau_v^2} + \frac{1}{6}\frac{t^3}{\tau_v^3} + ...\right) \approx v_0 t - \frac{1}{2}\frac{v_0}{\tau_v}t^2, \tag{3.2}$$

where the viscous time constant is $\tau_v = \frac{2}{9}\rho_L r_0^2/\mu_G$. At earlier times, the trajectory in equation (3.2) can be approximated by a second-order polynomial with a nearly constant deceleration rate of $-v_0/\tau_v$, which strictly speaking is the deceleration at the initial moment. Given these two limits, the departing velocity is therefore extrapolated from a second-order polynomial fit to the first three locations of the merged drop after its departure, $\tilde{z} = \tilde{z}(z_1, z_2, z_3, \delta t)$. The out-of-plane jumping velocity ($\bar{v}_z$)

reported in figure 3.3 was $\frac{d\tilde{z}}{dt}|_{z_1}$, the polynomial fit evaluated at the first captured location after the drop left the surface. The lower bound of the velocity measurement was given by by $\frac{z_2-z_1}{\delta t}$ which was solely based on experimental measurements. The upper bound was given by $\frac{d\tilde{z}}{dt}|_{\bar{r}_0}$ which was the polynomial fit evaluated at the average drop radius, approximately the lowest possible location for a departing merged drop (c.f. figure 3.1, $t = 2.67\,\mathrm{ms}$).

With our experimental setup, there was always some approaching velocity, but we ensured that we are in the low-Weber number regime, where the jumping velocity was not a function of the approaching velocity. For coalescence of large drops ($r_0 \gtrsim 300\ \mu\mathrm{m}$) on a Leidenfrost collider, the approaching velocity was usually on the same order with the jumping velocity. We further verify the insignificance of approaching velocity on the jumping velocity, by releasing the colliding drops at two different gate locations (see figure 2.1).

Unlike the colliding experiments, the exploding experiments had to be repeated over long periods of time to obtain desirable drop coalescence between two drops of approximately equal radii (within 15% difference). Data were only taken when the merging drops happened to be settled on the Leidenfrost surface, with the gap between the drop and surface comparable to the vapor layer thickness of static Leidenfrost drops. The in-plane velocity prior to coalescence was less than 0.05 m/s, significantly smaller than the out-of-plane jumping velocity which was above 0.1 m/s. Note that the data points between 200 μm and 350 μm in figure 3.3 are cases where two drops approached each other at very different approaching velocities, which results in a significant horizontal velocity after the drop jumped up. However, they still fall on the same curve. This range with similar approaching velocity can in principle be filled with the "exploder" mode, but is not the focus of our study.

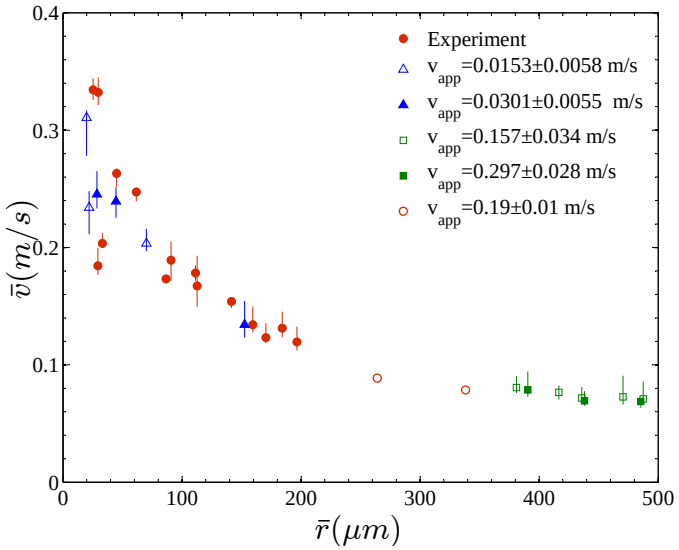

FIGURE 3.3: The jumping velocity of the merged drop is dependent on the average drop radius, but independent of the approaching velocity which is orthogonal to the jumping velocity. The disparity between the two drop radii was less than 15%. For large drops, the different approaching velocity were obtained by varying the location of the gates. The approaching velocity was measured when the two drops were at least one diameter away. For smaller drops, the approaching velocity was a result of the explosion and subsequent flotation of the small droplets; large approaching velocities were eliminated to avoid interference from the background vapor flow.

3.2 Limit of accessible drop radii

The experimentally accessible range of radii is roughly between 20 μm and 500 μm (figure 3.3). The upper bound is related to the capillary length, beyond which the drops are no longer spherical due to gravitational effects. The lower bound is due to the breakdown of the lubrication regime of the vapor layer intercalating the drop and the Leidenfrost surface, leading to departure of an *individual* drop from the heated substrate as shown in figure 3.4. The drop went up and down (before 0 ms) on the vapor layer for several cycles, each time to a slightly higher position and eventually launched off. A Leidenfrost drop is under mechanical equilibrium and remains on the surface when its gravity balances the lubrication pressure (Celestini et al., 2012). However, as the drop size decrease, vapor layer thickness increases which breaks the

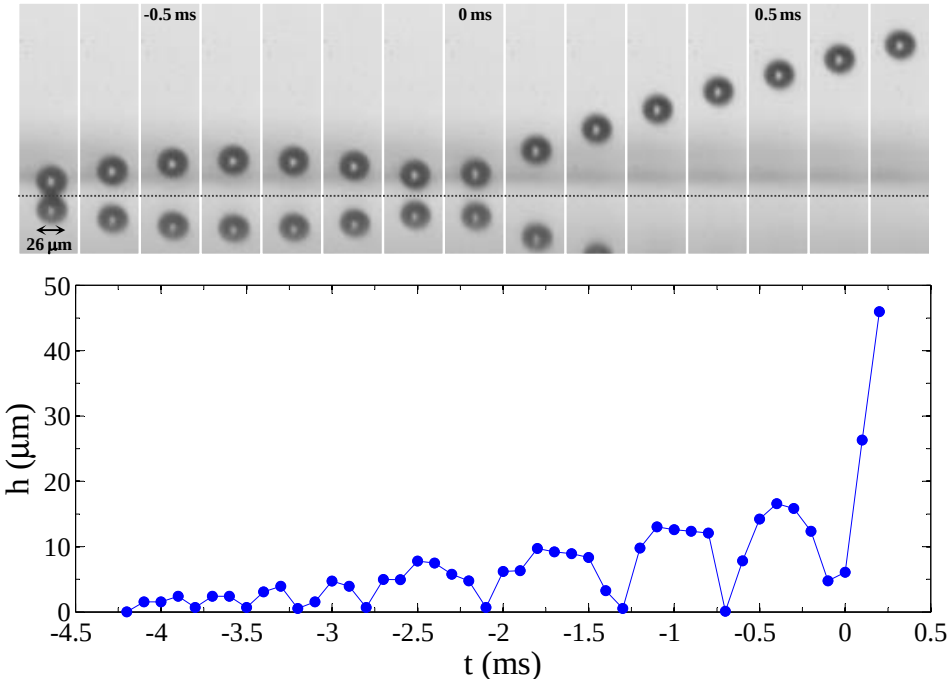

FIGURE 3.4: Spontaneous launching of a single Leidenfrost drop with a radius around 13 μm. The drop went up and down (before 0 ms) on the vapor layer for several cycles, each time to a slightly higher position and eventually launched off. Bottom image shows the distance of the drop from the substrate h (as defined in figure 1.1) as a function of time. The launching velocity is approximately 0.22 m/s.

balance between gravity and the upward pressure. The net upward force leads to the spontaneous jump of the single droplet.

4

Discussions

With the experimental results on Leidenfrost surfaces, we are now in a position to discuss the two puzzles of self-propelled jumping on superhydrophobic surfaces outlined in the introduction, namely the small non-dimensional jumping velocity and the cut-off radius around 30μm. We will also briefly report some experimental results on asymmetric coalescence.

4.1 Numerical model

The experimental data will be compared against numerical simulations of the jumping process. In collaboration with Professor James J. Feng's group at University of British Columbia, we have developed a 3D phase-field numerical model (to be reported elsewhere). In the numerical model, two adjacent drops initially are static with identical sizes and coalesce by interfacial diffusion on a non-wetting substrate with a contact angle of 180°. The experiments have shown that the approaching velocity does not change the jumping velocity when $We \leqslant 1$, so it is reasonable to neglect the approaching velocity in our numerical model. It is also important to note that we neglected the vapor layer between the Leidenfrost drops and the

heated substrate, as well as any active vaporization from the Leidenfrost drops. The evaporation is negligible during the quick jumping process. The entire process only lasts in the order of 10 ms as shown in figure 3.1 and 3.2, which is at least two orders of magnitude shorter than the lifetime of a Leidenfrost drop (Biance et al., 2003). To model the Leidenfrost coalescence, both liquid and air properties were taken as those at 1 atm and 100°C (the temperature inside the drop was measured to be 99±1°C) (Biance et al., 2003; Burton et al., 2012), except for the numerical air density which was approximately 20 times the physical value. Since this artificial air density was still much lower than that of water, we found that the discrepancy in air density was inconsequential to the numerical results such as the jumping velocities. In addition, gravity was neglected since the drop radii investigated here were significantly smaller than the capillary length (2.5 mm for water drops at 100°C).

The mechanism of jumping is revealed by the coalescence process in air shown in figure 4.1. When two drops coalesce in air, liquid bridge is formed to merge the initially distinct drops into one. The merged drop undergoes many cycles of capillary-inertial oscillations between oblate and prolate shapes, eventually relaxing to a larger spherical drop due to viscous effects. The dashed line indicates the position of an imaginary substrate. Had a non-penetrating physical substrate been present at the dashed line, the top-down symmetry of the oscillations would be broken and the merged drop would be forced to move upward as shown in figure 3.1. Note that the actual drop shape is more complex than a spheroid, in which case oblate and prolate are loosely referring to cases with the major axis parallel and perpendicular to the imaginary substrate, respectively.

From energetic point of view on the jumping process, the kinetic energy of the merged drop can be decomposed into two components, translational and oscillatory. The translational component comes from the substrate that breaks the top-down symmetry of energy release, giving rise to the velocity in the vertical direction. As

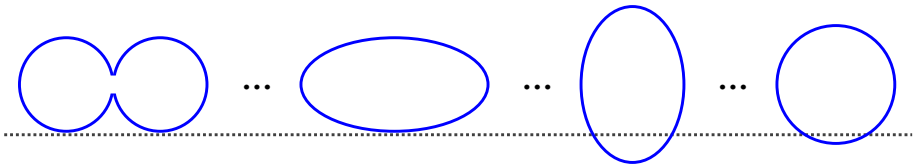

FIGURE 4.1: Schematic of drop coalescence process in air. The mechanism of jumping can be understood from the coalescence process in the air, without any substrate. A liquid bridge is formed to merge the initially distinct drops into one. The merged drop undergoes many cycles of capillary-inertial oscillations between oblate and prolate shapes, eventually relaxing to a larger spherical drop due to viscous effects. The dashed line indicates the position of an imaginary substrate. Had a non-penetrating physical substrate been present at the dashed line, the top-down symmetry of the oscillations would be broken and the merged drop would be forced to move upward.

shown in the simulations, the oscillatory component associated with the strong oscillation of coalescence process does not contribute to the vertical motion but is completely dissipated, which results in a much smaller energy conversion efficiency less than 4% from the released surface energy to the translational kinetic energy.

4.2 Jumping velocity

In this section, we will discuss the non-dimensional jumping velocity through comparison between Leidenfrost experiments and the numerical results (figure 4.2). The numerical jumping velocity was extracted as the departure velocity of the merged drop from a passive non-wetting surface. Both the experimental and numerical data followed the capillary-inertial scaling equation (1.1). The velocity increased with decreasing drop radius, roughly following a power law of $\bar{v} \sim r_0^{-1/2}$. The capillary-inertial scaling held for the experimentally accessible range of radii is roughly between 20 μm and 500 μm, with a non-dimensional velocity around 0.2, which is very close to that on superhydrophobic surfaces. Except for drop radii close to the lower bound of 20 μm, the jumping velocity consistently followed the numerical results at a slightly higher numerical value. This subtle but consistent discrepancy was likely a result of the dynamic role played by the vapor layer resulting from the hot Leidenfrost surface

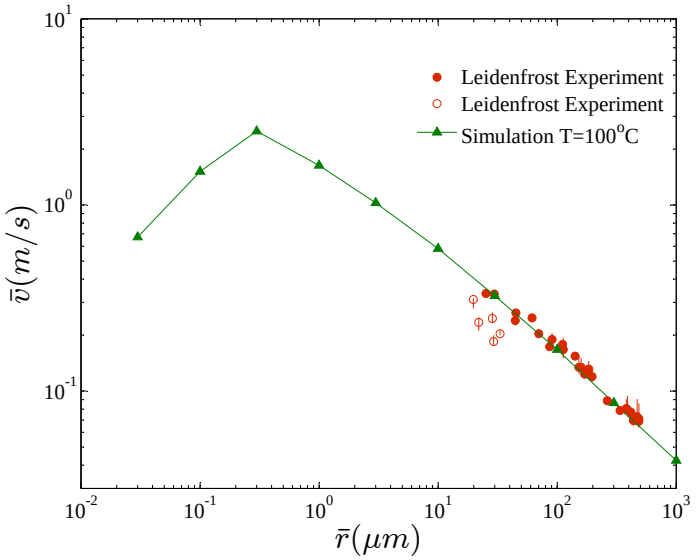

FIGURE 4.2: Comparison of experimental jumping velocities to simulations. Both experiments and simulations roughly follow the capillary-inertial velocity scaling with $\bar{v} \sim r_0^{-1/2}$. The quantitative agreement is excellent, except for very small radii at which the vapor layer thickness starts to fluctuate. The simulation result shows a cut-off at 100 nm.

(Biance et al., 2006), leading to slightly higher rebound velocity as the vapor layer was being compressed during the impact of the liquid bridge.

4.3 Cut-off radius

Based on the good agreement on the jumping velocity between our Leidnfrost experiment and the numerical model, we can now discuss the cut-off radius. The cut-off radius on superhydrophobic surface was observed to be around 30μm. However, no cut-off radius has been observed on Leidenfrost surfaces for the experimentally accessible drop radii down to 20μm . We should emphasize again that the deviation (hollow circles in figure 4.3 and 4.2) from the maximum jumping velocity is not indicative of a cut-off radius for the self-propelled jumping upon coalescence of a pair of drops, but rather the dynamic role played by the vapor layer (Section 4.2). Close to the lower bound of 20 μm, the thickness of the vapor layer between the drops and

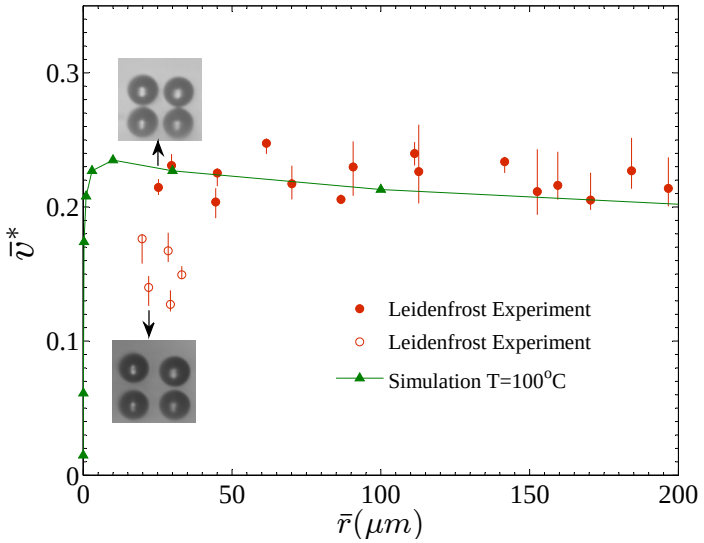

FIGURE 4.3: Comparison of nondimensional velocities to simulations. Cutoff radius for jumping in the numerical results cannot be experimentally accessed on Leidenfrost surfaces, on which no cutoff radius for jumping was observed. With initial drop radii below approximately 20 μm, the lubrication regime governing the vapor layer thickness broke down, and the thickness varied significantly as a consequence; see inset images for drops of comparable sizes captured at different instants. Excluding data points due to the fluctuations in the vapor layer thickness, the Leidenfrost experimental data closely followed the numerical predictions with a non-dimensiaonal velocity around 0.2. However, small drop radii could not be accessed because of the uncontrollable thickness of the vapor layer.

the heated substrate becomes uncontrollable because of the spontaneous movement of individual drops. As indicated by the insets in figure 4.3, thicker vapor layer consistently corresponds to lower jumping velocity. On superhydrophobic surface, the cut-off is most likely due to effects not captured by the simplified boundary condition of the non-wetting Leidenfrost surface, such as the drop-surface adhesion and interactions with cavities on the superhydrophobic surfaces.

Though we did not observed a cut-off radius in the Leidenfrost experiments, we captured a discrepancy in the cut-off radius between experiments on superhydrophobic surface and our numerical results. The numerical results for Leidenfrost drops (figure 4.2) show a clear cut-off at 100 nm, which is significantly smaller than 30μm

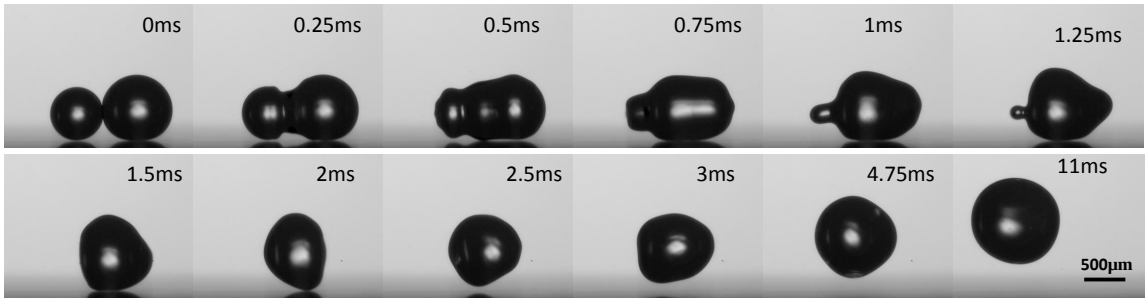

FIGURE 4.4: Asymmetric coalescence of Leidenfrost drops of disparate radii: 320 μm and 410μm respectively. The asymmetry in drop size brings in more complex coalescence process than symmetric coalescence. At departure point (2 ms), the contact area between the merged drop and the substrate is also much smaller than that in symmetric coalescence (2.67 ms in figure 3.1) The jumping velocity is measured to be around 0.06m/s and non-dimensional velocity is 0.14.

reported on a superhydrophobic surface. We may not be able to obtain coalescence for drops smaller than 20μm on Leidenfrost surfaces to reveal the source of discrepancy, due to the spontaneous launching of a single droplet below a critical radius (around 15μm for water drops on a 250°C Leidenfrost surface, calculated from equation (4) in Celestini et al. (2012)).

4.4 Asymmetric coalescence

The experimental data we have reported are within 15% radius difference which can be approximated as symmetric. However, asymmetric coalescence is more closely related to real applications mentioned in Chapter 1.

Now we will assess the effects of asymmetry in jumping velocity. A representative process for this asymmetric coalescence is shown in figure 4.4. The asymmetry in drop size brings in more complex coalescence process than symmetric coalescence (figure 3.1). At departure point (2 ms), the contact area between the merged drop and the substrate is also much smaller than that in symmetric coalescence (2.67 ms in figure 3.1).

The jumping velocity of asymmetric coalescence is compared with simulation in

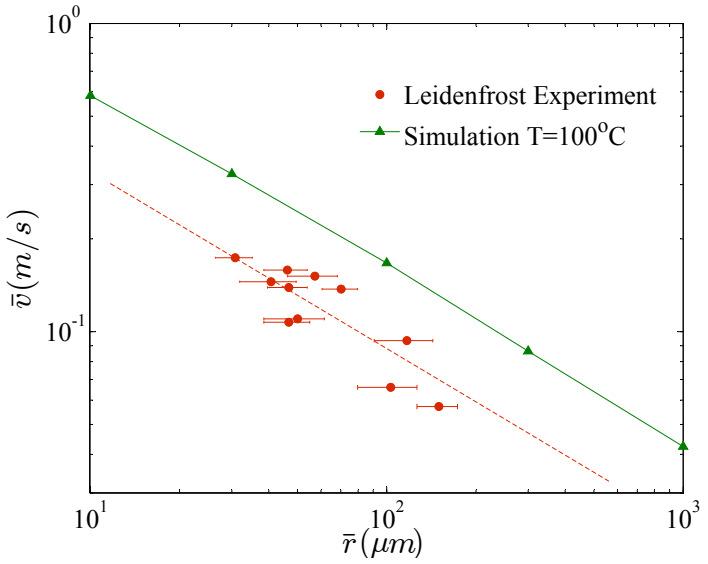

FIGURE 4.5: Jumping velocity of asymmetric coalescence of Leidenfrost drops. The center dots represents the average radius, while the left and right sides of error bars represents the small and the large drop radius respectively. The solid line is the simulation result for symmetric coalescence and the dashed line corresponds to non-dimensional velocity $\bar{v}^* = 0.12$.

figure 4.5. A clear lower velocity is observed for asymmetric coalescence compared to the numerical results for symmetric cases. Despite the large size difference, the asymmetric coalescence also follows capillary-inertial scaling, but with a smaller non-dimensional velocity (around 0.12, when non-dimensionalized by equation (1.1), with average radius of the two drops as r_0) than symmetric coalescence.

5

Conclusions

We studied the coalescence-induced jumping on non-wetting surface with Leidenfrost drops. The Leidenfrost drops have a contact angle of 180° with a vapor film lying beneath which eliminates the drop-surface adhesion and the complexity of moving contact lines on superhydrophobic surfaces. The measured jumping velocity for symmetric coalescence follows the capillary-inertial scaling with a non-dimensional velocity around 0.2, which is consistent with that on superhydrophobic surfaces. Asymmetric coalescence leads to a smaller jumping velocity but the trend is consistent with capillary-inertial scaling. Through comparisons with our phase-filed simulation, the capillary-inertial mechanism leading to self-propelled jumping is further confirmed. Unlike superhydrophobic surfaces, we did not observe an obvious cut-off for drop radii down to 20 μm, the lowest accessible to the Leidenfrost collider.

The self-propelled jumping on Leidnfrost surfaces and superhydrophobic surfaces share the same capillary-inertial scaling despite adhesion and moving contact lines on superhydrophobic surfaces. The results should also apply to self-propelled jumping upon coalescence on non-wetting surfaces in general, such as coalescence-induced jumping on *flat* surfaces for condensing mercury drops (Kollera and Grigull, 1969),

and on superhydrophobic surfaces for a sessile drop merging with an *incoming* drop (Farhangi et al., 2012).

For future work, the vapor layer thickness should be quantified and its dynamic role assessed both experimentally and theoretically (Snoeijer et al., 2009; Burton et al., 2012). The practically relevant case of asymmetric coalescence should be rigorously analyzed beyond the simple capillary-inertial scaling. The discrepancy of cut-off radius between experiments on superhydrophobic surfaces and numerical results should also be addressed. We cannot access smaller drops on Leidenfrost surfaces to resolve this, but possible alternatives can be condensation experiments on superhydrophobic surfaces with various patterns, which minimize the drop-surface adhesion (larger contact angle) and the interaction of the drop with the cavities (nano structure only). Those directions will hopefully lead to a more complete understanding of self-propelled jumping on Leidenfrost surfaces as well as other non-wetting surfaces.

Bibliography

Biance, A. L., Clanet, C., and Quéré, D. (2003), "Leidenfrost drops," *Phys. Fluids*, 15, 1632.

Biance, A. L., Chevy, F., Clanet, C., Lagubeauand, G., and Quéré, D. (2006), "On the elasticity of an inertial liquid shock," *J. Fluid Mech.*, 554, 47.

Boreyko, J. B. (2012), "From Dynamical Superhydrophobicity to Thermal Diodes," Ph.D. thesis, Duke University.

Boreyko, J. B. and Chen, C. H. (2009), "Self-Propelled Dropwise Condensate on Superhydrophobic Surfaces," *Phys. Rev. Lett.*, 103, 184501.

Boreyko, J. B. and Chen, C. H. (2010), "Self-propelled jumping drops on superhydrophobic surfaces," *Phys. Fluids*, 22, 091110.

Boreyko, J. B. and Chen, C. H. (2013), "Vapor chambers with jumping-drop liquid return from superhydrophobic condensers," *Int. J. Heat Mass Transfer*, 61, 409.

Boreyko, J. B. and Collier, C. P. (2013), "Delayed Frost Growth on Jumping-Drop Superhydrophobic Surfaces," *ACS nano*, 7, 1618.

Boreyko, J. B., Zhao, Y., and Chen, C. H. (2011), "Planar jumping-drop thermal diodes," *Appl. Phys. Lett.*, 99, 234105.

Burton, J. C., Sharpe, A. L., van der Veen, R. C. A., Franco, A., and Nagel, S. R. (2012), "Geometry of the vapor layer under a Leidenfrost drop," *Phys. Rev. Lett.*, 109, 074301.

Celestini, F., Frisch, T., and Pomeau, Y. (2012), "Take Off of Small Leidenfrost Droplets," *Phys. Rev. Lett.*, 109, 034501.

Chen, C. H., Cai, Q., Tsai, C., Chen, C. L., Xiong, G., Yu, Y., and Ren, Z. F. (2007), "Dropwise condensation on superhydrophobic surfaces with two-tier roughness," *Appl. Phys. Lett.*, 90, 173108.

Cheng, J., Vandadi1, A., and Chen, C. L. (2012), "Condensation heat transfer on two-tier superhydrophobic surfaces," *Appl. Phys. Lett.*, 101, 131909.

Dietz, C., Rykaczewski, K., Fedorov, A. G., and Joshi, Y. (2010), "Visualization of droplet departure on a superhydrophobic surface and implications to heat transfer enhancement during dropwise condensation," *Appl. Phys. Lett.*, 97, 033104.

Enright, R., Miljkovic, N., Al-Obeidi, A., Thompson, C. V., and Wang, E. N. (2012), "Condensation on Superhydrophobic Surfaces: The Role of Local Energy Barriers and Structure Length Scale," *Langmuir*, 28, 14424.

Farhangi, M. M., Graham, P. J., Choudhury, N. R., and Dolatabadi, A. (2012), "Induced Detachment of Coalescing Droplets on Superhydrophobic Surfaces," *Langmuir*, 28, 1290.

Feng, J., Pang, Y., Qin, Z., Ma, R., and Yao, S. (2012), "Why Condensate Drops Can Spontaneously Move Away on Some Superhydrophobic Surfaces but Not on Others," *ACS Appl. Mater. Interfaces*, 4, 6618.

He, M., Zhou, X., Zeng, X., Cui, D., Zhang, Q., Chen, J., Li, H., Wang, J., Cao, Z., Song, Y., and Jiang, L. (2012), "Hierarchically structured porous aluminum surfaces for high-efficient removal of condensed water," *Soft Matter*, 8, 6680.

Helbig, R., Nickerl, J., Neinhuis, C., and Werner, C. (2011), "Smart skin patterns protect springtails," *PloS ONE*, 6, e25105.

Kollera, M. and Grigull, U. (1969), "Über das Abspringen von Tropfen bei der Kondensation von Quecksilber," *Wärme-und Stoffübertragung*, 2, 31.

Miljkovic, N. and Wang, E. N. (2013), "Condensation heat transfer on superhydrophobic surfaces," *MRS Bulletin*, 38, 397.

Miljkovic, N., Enright, R., Nam, Y., Lopez, K., Dou, N., Sack, J., and Wang, E. N. (2013), "Jumping-Droplet-Enhanced Condensation on Scalable Superhydrophobic Nanostructured Surfaces," *Nano Lett.*, 13, 179.

Neitzel, G. P. and Dell'Aversana, P. (2002), "Noncoalescence and nonwetting behavior of liquids," *Ann. Rev. Fluid Mech.*, 34, 267.

Qian, J. and Law, C. K. (1997), "Regimes of coalescence and separation in droplet collision," *J. Fluid Mech.*, 331, 59.

Rykaczewski, K., Paxson, A. T., Anand, S., Chen, X., Wang, Z., and Varanasi, K. K. (2012), "Multimode Multidrop Serial Coalescence Effects during Condensation on Hierarchical Superhydrophobic Surfaces," *Langmuir*.

Snoeijer, J. H., Brunet, P., and Eggers, J. (2009), "Maximum size of drops levitated by an air cushion," *Phys. Rev. E*, 79, 036307.

Tang, C., Zhang, P., and Law, C. K. (2012), "Bouncing, coalescence, and separation in head-on collision of unequal-size droplets," *Phys. Fluids*, 24, 022101.

Watson, J. A., Cribb, B. W., Hu, H. M., and Watson, G. S. (2011), "A dual layer hair array of the brown lacewing: repelling water at different length scales," *Biophys. J.*, 100, 1149.

Wisdom, K. M., Watson, J. A., Qu, X., Liu, F., Watson, G. S., and Chen, C. H. (2013), "Self-cleaning of superhydrophobic surfaces by self-propelled jumping condensate," *PNAS*, p. 7992.

Zhang, Q., He, M., Chen, J., Wang, J., Song, Y., and Jiang, L. (2013), "Anti-icing surfaces based on enhanced self-propelled jumping of condensed water microdroplets," *Chem. Commun.*, 49, 4516.